Two-Coordinate, Non-Linear Vanadium(II) and Chromium(II) Complexes of the Silylamide Ligand – $N(SiMePh_2)_2$: Characterization and Confirmation of Orbitally Quenched Magnetic Moments in Complexes with Sub-d^5 Electron Configurations

Kerstin Freitag,† Cary R. Stennett,‡ Akseli Mansikkamäki,ǁ,* Roland A. Fischer,†,* and Philip P. Power‡,*

†Inorganic and Metalorganic Chemistry, Technical University Munich, D-85748, Garching, Germany

‡ Department of Chemistry, University of California, Davis, One Shields Avenue, Davis, California 95616, United States

ǁ NMR Research Unit, Faculty of Science, University of Oulu, P.O. Box 3000, Oulu, FIN-90014, Finland

Abstract.

The two-coordinate metal amide complexes $V\{N(SiMePh_2)_2\}_2$ (**1**) and $Cr\{N(SiMe_2Ph)_2\}_2$ (**2**) were synthesized by reaction of two equivalents of $LiN(SiMePh_2)_2$ with $VI_2(THF)_4$ or $CrCl_2(THF)_2$ in *n*-hexane. Their crystal structures showed that they have bent coordination, N-V-N = 137.0(4)°, N-Cr-N = 139.19(5)°, at the metals. The vanadium complex (**1**) displayed no tendency to isomerize as previously observed for some V(II) amido complexes. Curie fits of SQUID magnetic measurements afforded magnetic moments of 3.36 (**1**) and 4.68 (**2**) μ_B, consistent with high-spin configurations. These values are lower than the spin-only values of 3.88 and 4.90 μ_B expected for d^3 and d^4 complexes, suggesting a significant unquenched orbital angular momentum contribution to the overall moment, which is lower as a result of the positive spin-orbit coupling constants.

Introduction

Sterically encumbering silylamido ligands have featured prominently in the chemistry of low-coordinate and low-valent transition metal chemistry since the outset of research in this area. Beginning with the pioneering work of Bürger and Wannagat in the early 1960s, the bis(trimethylsilyl)amide ligand was shown to stabilize low-coordinate first row transition metal amide complexes in their +2 (Mn, Co, and Ni) and +3 (Cr and Fe) oxidation states.[1,2] Structural studies of these complexes later indicated that the pure divalent species existed as three-coordinate, amide bridged dimers,[3–5] and that the tervalent complexes are three-coordinate monomers,[6–11] showing that the $-N(SiMe_3)_2$ ligand is incapable of stabilizing neutral two-coordinate monomeric complexes of these metals in the solid state. In the late 1980s, however, it was shown that the increased bulk of the commercially available silylamide ligand $-N(SiMePh_2)_2$ enforced stabilization of monomeric, quasi two-coordinate complexes of divalent iron, cobalt (the first examples of such complexes for these metals), and manganese.[12,13]

Despite the demonstrated ability of the $-N(SiMePh_2)_2$ ligand to produce low-coordination in the later transition metals, two-coordinate complexes of early transition metals featuring this ligand remain unknown. Indeed, two-coordinate molecular complexes of divalent vanadium and chromium are exceptionally rare.

Only four such complexes are known for vanadium (the first of which was not reported until 2013),[14,15] although several low-valent complexes of higher coordination at vanadium are known.[8,15–19] Neutral two-coordinate complexes of chromium are more numerous, with ca. a dozen such complexes now reported.[15,20–27] The paucity of two-coordinate complexes of these metals, particularly vanadium, is likely due to the difficulty involved in preparing appropriate divalent metal halide complexes as precursors. The difficulty in isolating these complexes is further highlighted by the ability of two-coordinate vanadium complexes to isomerize to other coordination modes when bulky amide ligands previously shown to stabilize two-coordinate complexes of other metals are used (e.g. -N(Si^{i}Pr$_3$)Dipp, Dipp = 2,6-diisopropylphenyl).[15]

Because of these difficulties, investigations of the chemistry and properties of two-coordinate open-shell (d^1-d^9) transition metal complexes have mainly focused on species in which the d-valence shell is at least half full (i.e. d^5-d^9).[28] Other reasons for this circumstance include the wide availability of divalent metal halide salts of the later transition metals, as well as the smaller size of the metal ions which makes it easier to obtain the low-coordination numbers by steric blocking. In addition, the magnetic properties of the later, two-coordinate complexes, particularly the d^6 and d^7 Fe(II) and Co(II) complexes, have demonstrated that they can possess very high magnetic moments which arise from unquenched orbital contributions and large negative spin-orbit coupling constants in which the spin and orbital moments combine to give a moment that is significantly greater than the spin only value.[29–33] Furthermore, high axial zero field splitting is often present, which makes the complexes interesting from the aspect of single molecule magnetism.[32,33] These properties, coupled with the increasingly high temperature magnetic hysteresis displayed by lanthanide complexes, effectively allows the magnetic properties of a complex to be tuned by judicious choice of metal or ligand.[34–37]

However, in complexes with less than half-filled valence shells (i.e. d^1-d^4), the spin-orbit coupling is positive and the orbital moments act in such a way to oppose the spin moments.[38] Yet, there are comparatively few studies of this phenomenon in the two-coordinate complexes of earlier transition metals.[14,15,27] For these metals, the divalent state is generally more difficult to access, and the sizes of metal(II) ions are significantly larger, making it more difficult to stabilize two-coordination.[39] As a result, there are few detailed magnetic studies of these systems.[14,15,27] Herein, we demonstrate that two-coordinate complexes of vanadium and chromium are accessible in acceptable yields and in a facile manner from the reaction of easily-prepared metal halide salts with commercially available ligands. In addition, we show that their magnetic moments are lower than the spin only values, a result of their less than half-filled valence shell. These findings constitute rare examples of manifestations of the moment decreasing spin-orbit effect in a first-row transition metal complex due to the positive value of the spin-orbit coupling constant, λ.

Experimental

General. All manipulations were carried out in an atmosphere of purified argon using standard Schlenk and glovebox techniques. Hexane was dried using an MBraun solvent purification system. The

final water content in all solvents was checked by Karl Fischer titrations. Elemental analyses were performed by the Kolbe Microanalytics Laboratory, Mülheim an der Ruhr, Germany. Deviations in the elemental analyses are typical of metal amide complexes, particularly those with high silicon content.[9,40,41] UV–vis spectra were recorded as dilute hexane (**1**) or diethyl ether (**2**) solutions in 3.5 mL quartz cuvettes using an OLIS modernized Cary 14 UV/vis/NIR spectrophotometer (**1**) or a Perkin-Elmer UV/VIS/NIR spectrometer (**2**). Infrared spectra were recorded using a Bruker Alpha FTIR spectrometer under an argon atmosphere in a glovebox. $CrCl_2(THF)_2$,[42] $VI_2(THF)_4$,[43] and $LiN(SiMePh_2)_2$[12] were prepared according to literature procedures. All other materials were commercially obtained and used as received.

Synthesis of V{N(SiMePh$_2$)$_2$}$_2$ (**1**). $VI_2(THF)_4$ (0.100 g, 0.168 mmol) was suspended in 10 mL of hexanes and cooled to *ca.* – 30 °C. $LiN(SiMePh_2)_2$ (0.140 g, 0.336 mmol) suspended in 10 mL hexanes was added dropwise to the $VI_2(THF)_4$ suspension. The reaction mixture was slowly warmed to room temperature. After stirring at ambient temperature for 30 minutes, the reaction mixture became brown. After 24 h a dark red/brown reaction mixture with a white precipitate had formed. The solution was filtered, and the filtrate was concentrated to 5 mL under reduced pressure and stored at 5 °C. Dark red crystals suitable for single crystal X-ray diffraction grew within 24 hours. Yield 0.045 g (31 %). Calc. for $C_{52}H_{52}VN_2Si_4$ (%): C 71.93, H 6.04, N 3.23, Si 12.94, V 5.86; Found: C 65.28, H 5.79, N 2.85, Si 11.90, V 5.25. UV-Vis: λ_{max} 430 nm (ε = 9000 $M^{-1}\,cm^{-1}$) IR: 3039-2932 (νC-H), 1414 (νC-H), 1234 (νSi-CH_3), 1095 (νC-H), 410 (νV-N).

Synthesis of Cr{N(SiMePh$_2$)$_2$}$_2$ (**2**). $CrCl_2(THF)_2$ (0.250 g, 0.936 mmol) was suspended in 15 mL of hexanes and cooled in an ice bath to *ca.* 0 °C. $LiN(SiMePh_2)_2$ (0.780 g, 1.872 mmol) suspended in 15 mL of hexanes was added dropwise to the $CrCl_2(THF)_2$ suspension. The reaction mixture turned green/yellow immediately and was slowly warmed to room temperature. After four hours at ambient temperature a white precipitate had formed, and the green solution was filtered. The filtrate was then concentrated to 5 mL under reduced pressure and stored at ca. 5 °C. Yellow plates suitable for single crystal X-ray diffraction grew within 24 hours. Yield 0.46 g (57 %). Calc. for $C_{52}H_{52}CrN_2Si_4$ (%): C 71.84, H 6.03, N 3.22, Si 12.92, Cr 5.98; Found: C 70.82, H 6.34, N 3.26, Si 12.72, Cr 5.87. UV-Vis: λ_{max} 365 nm. IR: 3040-2934 (νC-H), 1413 ν(C-H), 1234 (νSi-CH_3), 378 (νCr-N).

X-ray Crystallography. Single crystals of **1** and **2** that were suitable for diffraction studies were obtained from concentrated hexane solutions at 5 °C after one day. The X-ray intensity data for **1** and **2** were collected on an Agilent Technologies SuperNova diffractometer with an Atlas CCD detector and Cu K_α radiation (1.54178 Å) from a microfocus X-ray source with multilayer X-ray optics. Suitable crystals were coated with a perfluoropolyether, mounted on a nylon cryo loop, and immediately positioned in a low temperature (100 K) stream of nitrogen. The data were processed using the CrysAlisPro software suite.[44] Absorption corrections based on multiple-scanned reflections were carried out using ABSPACK.[45] The crystal structures were solved by direct methods using SHELXS-97 and refined with SHELXL-2014.[46] The positions of all non-hydrogen atoms were refined anisotropically.

Magnetic Measurements. Magnetic susceptibility data were recorded at the Max Planck Institute for Chemical Energy Conversion with powder samples of solid material in the temperature range 2-300K using a superconducting quantum interference device (SQUID) susceptometer with a field of 1.0 T (MPMS-7, Quantum Design, calibrated with standard palladium reference sample, error < 2 %). Variable-temperature magnetization measurements were taken at 1 T in the range 2-300K with the magnetization sampled on a linearized 1/T temperature scale. The experimental data were corrected for underlying diamagnetism using tabulated Pascal's constants as well as for temperature-independent paramagnetism (TIP).[47]

Results and Discussion

Synthesis. Highly air and moisture sensitive complexes $V\{N(SiMePh_2)_2\}_2$ (**1**) and $Cr\{N(SiMePh_2)_2\}_2$ (**2**) were synthesized via salt metathesis (Scheme 1) of the lithium amide and the corresponding metal halide. Addition of $LiN(SiMePh_2)_2$ to $VI_2(THF)_4$ at -30 °C gives an initially pale green reaction mixture that begins turning orange after stirring at room temperature for 30 minutes, with moderate yields being obtained after 24 hours. In contrast, slow addition of the lithium silyl-amide to $CrCl_2(THF)_2$ immediately resulted in a color change of the initial pale blue reaction mixture to green/yellow. A short reaction time of four hours resulted in a reproducibly good yield. The described routes are straightforward and afford the highest yields. A peculiarity of the syntheses is that they were conducted in hexane in contrast to the typically used ether solvents. The use of hexane emerged from the testing of different solvents such as diethyl ether, toluene, and tetrahydrofuran as solvents for both reactions, with hexane giving the best yields. The formation of THF complexes was not observed in either case.

Scheme 1: Synthetic routes for 1 and 2

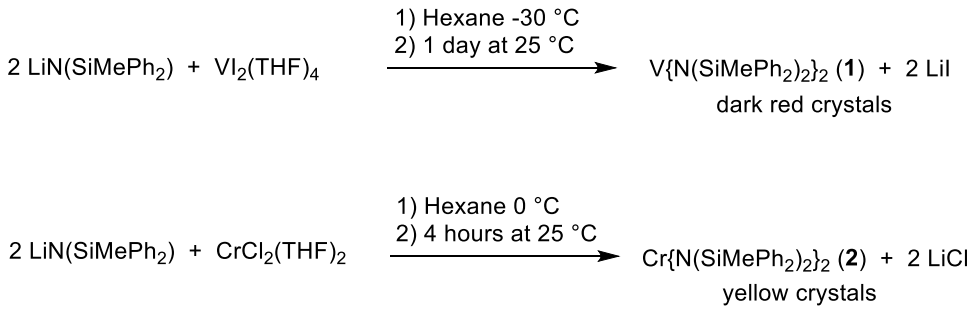

Structures. The molecular structures of compounds **1** and **2** are depicted in Figure 1 and Figure 2. Selected bond lengths and angles are given in Table 1 along with the comparable values for the analogous iron and cobalt bis(silylamides).[12] Complex **1** crystallizes in the monoclinic space group $P2_1/c$ with four molecules in the unit cell. The vanadium bis(silylamide) has a bent coordination geometry with a N1-V1-N2 angle of 137.04(6)°). This angle is somewhat wider than that found in $V\{N(H)Ar^{Me6}\}_2$ (N-V-N: 123.47(9)), the only other reported vanadium(II) bis(amide) having bent geometry.[9] A phenyl ring from each ligand is directed towards the vanadium atom, resulting in short $V\text{-}C_{phenyl}$ distances (V1···C21 2.447(1) Å,

V1···C34 2.488(1) Å). These distances are within the reported range of secondary interactions of phenyl rings in two coordinate aryl amide complexes of vanadium (cf. the shortest V-C_{aryl} distances in $V\{N(H)Ar^{iPr6}\}_2$ (V-C_{aryl}: 2.5330(13)), $V\{N(H)Ar^{Me6}\}_2$ (V-C_{aryl}: 2.463(2)), and $V\{N(Si^iPr_3)Dipp\}_2$ (V-C_{aryl}: (2.3024(5)), (Ar^{iPr6} = C_6H_3-2,6-(C_6H_2-2,4,6-$^i Pr_3$)$_2$, Ar^{Me6} = C_6H_3-2,6-(C_6H_2-2,4,6-Me_3)$_2$, Dipp = 2,6-diisopropylphenyl)).[14,15] The direction of the phenyl rings towards the central metal atom again results in varying V-N-Si bond angles in the range of 101.05(9) (V1-N1-Si2) to 135.66(8)° (V1-N2-Si4). The V-N bond distances of 2.004(1) (V1-N1) and 2.012(1) Å (V1-N2) are comparable to the three known two-coordinate vanadium amides mentioned above, which range from 1.992(1) – 1.976(2) Å.[14,15] The latter vanadium(II) complex, $V\{N(Si^iPr_3)Dipp\}_2$, which was recently reported by Tilley and coworkers, has linear coordination in the solid state but isomerizes in solution into a metallocene complex formed by breaking of the two V-N bonds and formation of a sandwich complex with η^5 bonding between vanadium and the aryl groups of the two ligands.[15] While complex **1** is rich with aryl groups capable of supporting such a complex, the absence of an N-C_{aryl} bond capable of forming an imide moiety in the ligand renders such an isomerization unlikely.

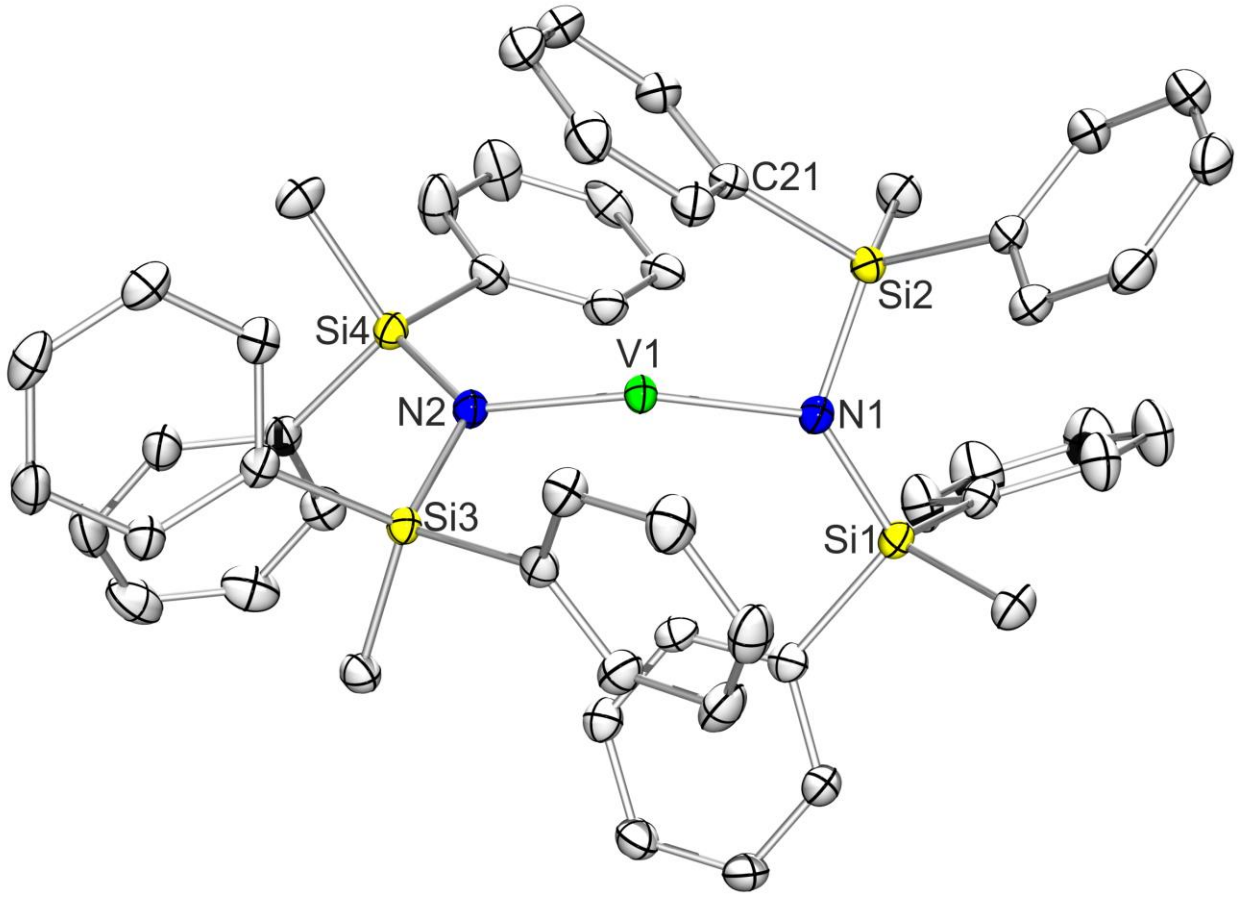

Figure 1: Molecular structure of **1** as determined by single crystal X-ray diffraction. Displacement ellipsoids are drawn at the 50 % probability level. Hydrogen atoms are not shown for clarity. Selected bond angles and distances are given in Table 1.

Complex **2** crystalizes in the triclinic space group $P\bar{1}$ with two molecules in the unit cell. The molecule has a bent coordination geometry with a N1-Cr1-N2 angle of 139.19(5)°, which is narrower than those observed for Fe{N(SiMePh$_2$)$_2$}$_2$ (N1-Fe-N2 169.0(1) °) and Co{N(SiMePh$_2$)$_2$}$_2$ (N1-Co-N2 147.0(1)°).[12] However, the bond angle is similar to that in the recently published complex Cr{N(SiMe$_2$Ph)$_2$}$_2$ (N1-Cr-N2 140.89(4) °).[22] More extreme bending of the coordination geometry is also known for two coordinate arylamide complexes such as Cr{N(H)Ar^{Me6}}$_2$ (N1-Cr-N2 121.49(3) °).[27] In contrast to complex **1**, complex **2** has only a single short Cr-C$_{phenyl}$ approach (Cr···C21 2.359(1) Å), indicating secondary interactions between the central metal atom and the phenyl ring. This type of interaction has also been observed in M{N(SiMePh$_2$)$_2$}$_2$ (M = Fe, Co), which were the first structurally characterized examples of two-coordinate complexes of these metals. However, the respective M-C$_{phenyl}$ distances are slightly elongated (2.585(7) – 2.695(5) Å).[12] As a consequence, the Cr-N-Si angles in **2** range between 98.44(6) (Cr1-N1-Si2) and 127.30(7)° (Cr1-N1-Si1). The Cr-N bond lengths of 1.963(1) and 2.016(1) Å differ by ca. 0.05 Å but both distances are in within the range of Cr-N bond lengths of known two-coordinate chromium(II) amides (1.943(3)-2.0036(1) Å).[20,22–24,27] The contraction of the shorter Cr-N1 bond length in comparison to the Cr-N2 bond length is associated with the secondary interaction between chromium and an aryl carbon (C21) of the same ligand.

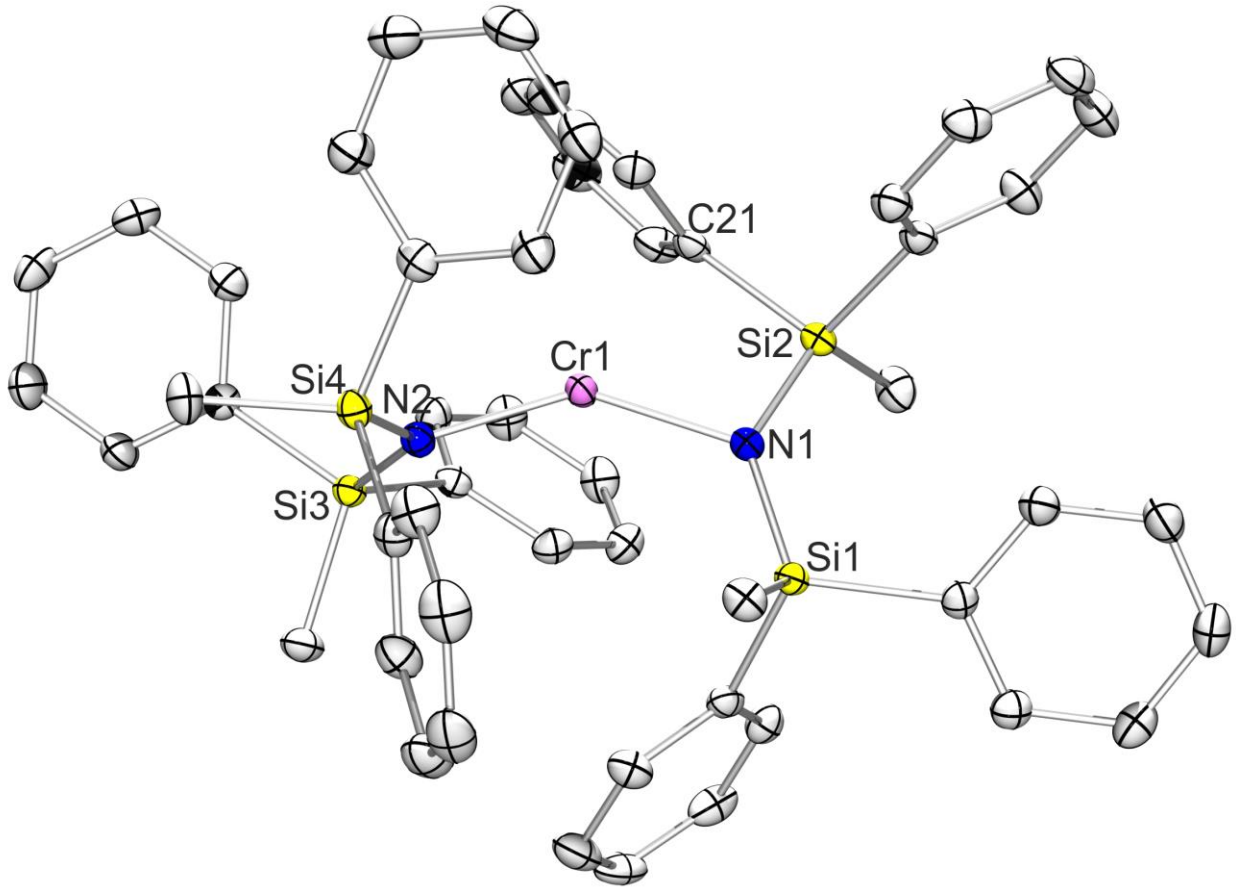

Figure 2: Molecular structure of **2** as determined by single crystal X-ray diffraction. Displacement ellipsoids are drawn at the 50 % probability level. Hydrogen atoms are not shown for clarity. Selected bond angles and distances are given in Table 1.

Table 1. Selected interatomic distances (Å) and angles (°) for 1, 2 and M{N(SiMePh$_2$)$_2$}$_2$ (M = Fe, Co).

	V{N(SiMePh$_2$)$_2$}$_2$ (1)	Cr{N(SiMePh$_2$)$_2$}$_2$ (2)	Fe{N(SiMePh$_2$)$_2$}$_2$[12]	Co{N(SiMePh$_2$)$_2$}$_2$[12]
M-N1	2.004(1)	1.963(1)	1.916(2)	1.898(3)
M-N2	2.012(1)	2.016(1)	1.918(2)	1.904(3)
M···C$_{Phenyl}$	2.447(1) (C21) 2.488(1) (C34)	2.359(1) (C21)	2.695(5) (C14)	2.588(7) (C7) 2.584(7) (C27)
N1-M-N2	137.04(6)	139.19(5)	169.0(1)	147.0(1)
M-N1-Si1	132.59(8)	127.30(7)	121.9(1)	103.8(2)
M-N1-Si2	101.05(7)	98.44(6)	106.1(1)	130.7(2)
M-N2-Si3	101.05(7)	115.20(7)	117.8(1)	103.0(2)
M-N2-Si4	135.66(8)	116.81(7)	115.0(1)	130.2(2)

Electronic Spectroscopy. Complexes **1** and **2** each display a single absorbance in the UV-vis spectra at 430 and 365 nm, respectively, consistent with their red (**1**) and yellow (**2**) colors. The intensity of these absorbances is consistent with their assignment as charge transfer bands. Upon crystallization, complexes **1** and **2** display poor solubility in hydrocarbon solvents, a characteristic which precluded the preparation of samples of sufficient concentration to observe any potential d-d transitions.

Magnetic Properties. The static magnetic susceptibilities of **1** and **2** show Curie behavior at higher temperatures (Figure 3). Slight deviations in the high-temperature range, especially for **1**, can be explained by trace of impurities, possibly due to decomposition of the highly sensitive compounds. In case of **1** the Curie behavior is observed above a temperature of about 15 K. At lower temperatures, a sharp drop in the χT product is observed which most likely originates from the thermal depopulation of states in the zero-field split ground spin-multiplet. A Curie fit between 15 and 300 K leads to an effective magnetic moment of 3.36 μ_B. Similarly, the magnetic susceptibility of **2** displays Curie behavior above a temperature of about 50 K. A Curie fit of the susceptibility between 50 and 300 K gives an effective magnetic moment of 4.68 μ_B. Below the temperature of 50 K, a sharp increase in the χT product of **2** is observed. This cannot be assigned to zero-field splitting of the ground spin-multiplet, but most likely originates from some form of magnetic ordering taking place due to intermolecular interactions. However, the closest approach between chromium atoms in the crystal structure of **2** is 10.505 Å, which would make magnetic ordering by dipolar interactions unlikely. Furthermore, the distances between the V(II) ions in **1** are similar and no appreciable ordering is

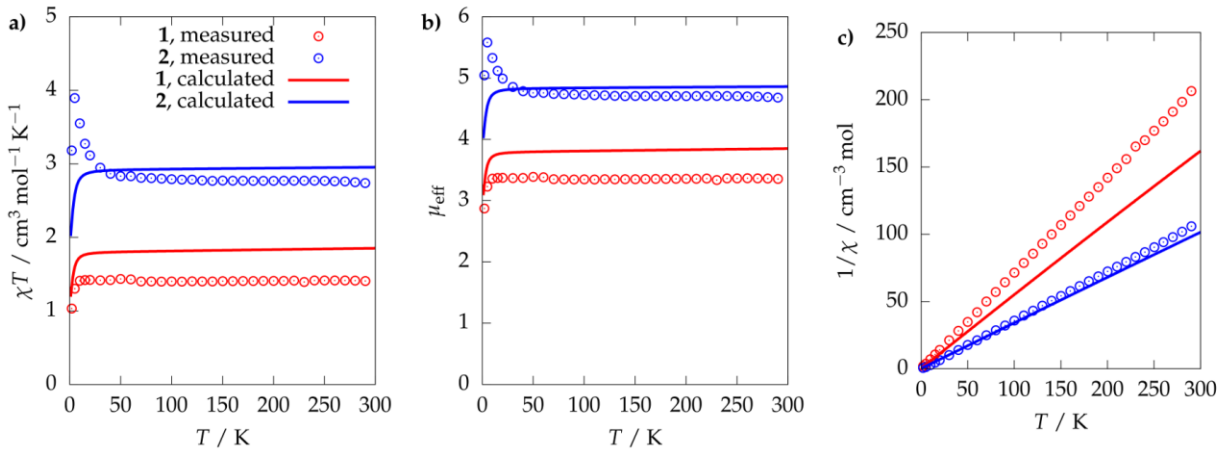

Figure 3: Measured and calculated static magnetic susceptibility (a), effective magnetic moment (b) and inverse susceptibility (c) of **1** and **2**.

observed in the respective susceptibility. The most plausible explanation is that a change in the crystal structure of **2** at low temperature that allows shorter intermolecular contacts.

The ground multiplets of V(II) and Cr(II) are $^4F_{3/2}$ and $^5D_0$, respectively. Within *LS* coupling, the respective spin-orbit coupled magnetic moments $\mu = g_J(J(J+1))^{1/2}\mu_B$ are 0.77 μ_B and 0.00 μ_B.[38,48] In a crystal field that lifts all degeneracies and fully quenches the orbital contributions to the angular momenta, the magnetic momenta should be reduced to near spin-only values of $\mu = g_e(S(S+1))^{1/2}\mu_B$ of 3.88 μ_B and 4.90 μ_B, for V(II) and Cr(II), respectively. In the case of both V(II) (d^3) and Cr(II) (d^4), the open 3*d* shell is less than half-filled giving rise to a positive spin-orbit coupling constant. This leads to partial cancellation of the free-ion orbital and spin magnetic moments, and to total momenta that are less than the spin-only values. The effective magnetic moments observed for **1** and **2** are slightly smaller than the respective spin-only values but are much closer to them than to the free-ion values. This corresponds to a case where the first order orbital contribution to the magnetic moment is essentially quenched while second-order contributions reduce the observed effective magnetic moments below the spin-only values.

The small deviation of the effective magnetic moments of complexes **1** and **2** from their spin-only values indicates that the quenching of the angular momentum is strong. In an ideal linear crystal-field with $D_{\infty h}$ symmetry, the d^3 electronic configuration of a V(II) ion of **1** should give a $^4\Pi_g$ state with a two-fold orbital degeneracy. This should lead to strongly anisotropic unquenched orbital contribution to the moment. The efficient quenching of this moment can be attributed to bending of the metal coordination, which lifts the two-fold orbital degeneracy. In addition, the relatively short V-C interactions (2.447(1) Å (V-C21) and 2.4888(1) Å (V-C34) may also contribute to quenching the orbital moment. However, the observed moment of **1** is very close to the value 3.41 μ_B measured for V{N(H)Ar^{Pri6}}$_2$, which has an almost linear (N–V–N = 179.98(7)°) N–V–N angle and a V–C interaction of 2.5330(13) Å. Neither of these μ_B values is as low as the 2.77 μ_B observed in V{N(H)Ar^{Me6}}$_2$, which has a strongly bent structure with two vanadium sites, one of which interacts strongly with a flanking aryl ring from the terphenyl ligand (shortest V-C$_{phenyl}$ distance: 1.839

Å).[14] These magnetic data indicate that the quenching cannot be unambiguously assigned to either the bending or the flanking metal–aryl interaction. For the Cr(II) complex **2**, in an ideal linear crystal-field, the d^4 electronic configuration of the Cr^{II} ion should give rise to an orbitally non-degenerate $^5\Sigma_g$ state. Thus, the orbital moment is perfectly quenched to first order. The orbital moment can, however, make a significant second order contribution, as is most likely observed in the case of **2**. Although the overall reduction in magnetic moment is not as great as previously observed (cf. μ_{eff} = 4.2 - 4.36 μ_B for $Cr\{N(H)Ar^{Me6}\}_2$, $Cr\{N(H)Ar^{Pri4}\}_2$, or $Cr\{N(H)Ar^{Pri6}\}_2$), it is nonetheless present and in agreement with our previous observations for these low-coordinate complexes.[27]

Theoretical calculations. The electronic structures of **1** and **2** were modeled using multireference electron correlation methods at NEVPT2//SA-CASSCF level of theory.[49–55] Before the inclusion of spin-orbit coupling (SOC), the ground state of **1** is an energetically well-separated spin-quartet state. The first excited quartet state lies 4844 cm^{-1} above the ground state, while the lowest state with a lower multiplicity is a spin-doublet at 9335 cm^{-1}. Once SOC is taken into account, the ground state is weakly split by SOC due to mixing with the excited spin states. The splitting can be described by zero-field splitting (ZFS) parameters D = +3.6 cm^{-1} and E = 0.4 cm^{-1}. The principal components of an effective **g** matrix of the ground multiplet were calculated as g_x = 1.927, g_y = 1.951 and g_z = 1.996. The values are smaller than the free-electron g-factor consistent with a magnetic moment that has been reduced in comparison to its spin-only value. In the case of **2**, before inclusion of SOC, the ground state is a spin-quintet separated from the first excited quintet state by 4615 cm^{-1} and the lowest triplet state lies 15047 cm^{-1} above the ground state. The calculated ZFS parameters are D = –2.7 cm^{-1} and E = 0.2 cm^{-1} leading to a very similar energy level structure to that of **1**. The principal components of an effective **g** matrix were calculated as g_x = 1.936, g_y = 1.987 and g_z = 1.995, again consistent with a reduced magnetic moment. The negative sign of the axial D parameter could, in principle, lead to slow relaxation of magnetization in **2**. However, the small absolute value of the D parameter and the relatively large E parameter, as compared to the D parameter, would lead to both a low effective barrier and efficient spin-phonon and quantum tunnelling mechanisms for the relaxation of magnetization. As a result, the magnetization dynamics were not studied further. Overall, the calculated electronic structure is in full agreement with conclusions made based on the magnetic measurements.

The magnetic susceptibility of both **1** and **2** was modeled based on the computational results and is included in Figure 3. In both cases, the susceptibility is somewhat overestimated in comparison to the measured susceptibility. This result is due to the over-stabilization of high-spin states in the SA-CASSCF calculations due to the understimation of metal–ligand covalency.[56] In case of **1**, the calculated susceptibility is qualitatively similar to the experimental plot. A Curie fit of the calculated susceptibility in the same temperature range as the experimental susceptibility leads to an effective magnetic moment of 3.85 μ_B. The value is somewhat higher than the experimentally measured value and is very close to the spin-only value. In case of **2**, the calculated susceptibility differs qualitatively from the experimental susceptibility mainly in

the low-temperature region. This is consistent with the possibility that the rise in the experimental susceptibility originates from intermolecular interaction or from changes in the crystal-structure as neither possibility can be considered in the calculations. A Curie-fit of the susceptibility data in the same temperature range as the experimental data leads to an effective magnetic moment of 4.87 μ_B, which is again higher than the experimentally determined value and close to the spin-only value, while still slightly smaller.

The splitting of the 3*d* orbitals under the effects of the crystal field was further studied by *ab initio* ligand field theory.[57,58] In an ideal linear crystal field, the 3*d* orbitals are split into a doubly degenerate δ set consisting of the $3d_{x2-y2}$ and $3d_{xy}$ orbitals, a doubly degenerate π set consisting of the $3d_{xz}$ and $3d_{yz}$ orbitals and a non-degenerate σ level consisting of the $3d_{z2}$ orbital. The δ set should lie the lowest in energy and the σ orbital should be the highest. The calculated effective ligand field orbitals (Figure 4) do not show any of the degeneracies associated with an ideal linear crystal field. For **1**, the orbital ordering is the same as what would be predicted for an ideal linear complex. However, the near-degenerate sets of π and a δ orbitals do not contribute any first-order angular momentum. In complex **2**, the δ set is split by only 795 cm^{-1} thus retaining a quasi-degenerate structure, while the π set is more strongly split. Compared to an ideal linear crystal field also the order of one of the π orbitals and the σ orbital is reversed. Thus, while **1** and **2** are two-coordinate, the deviations from linear coordination and the flanking metal–aryl interactions destroy the resemblance to the orbital structure in a linear geometry. This explains the strong quenching of the orbital contributions to the angular momentum. The effective SOC constants of **1** and **2** were calculated as 153 cm^{-1} and 220 cm^{-1}, respectively. The values are much smaller than the splitting between the ground and first excited states, thereby explaining the weak mixing of states under SOC.

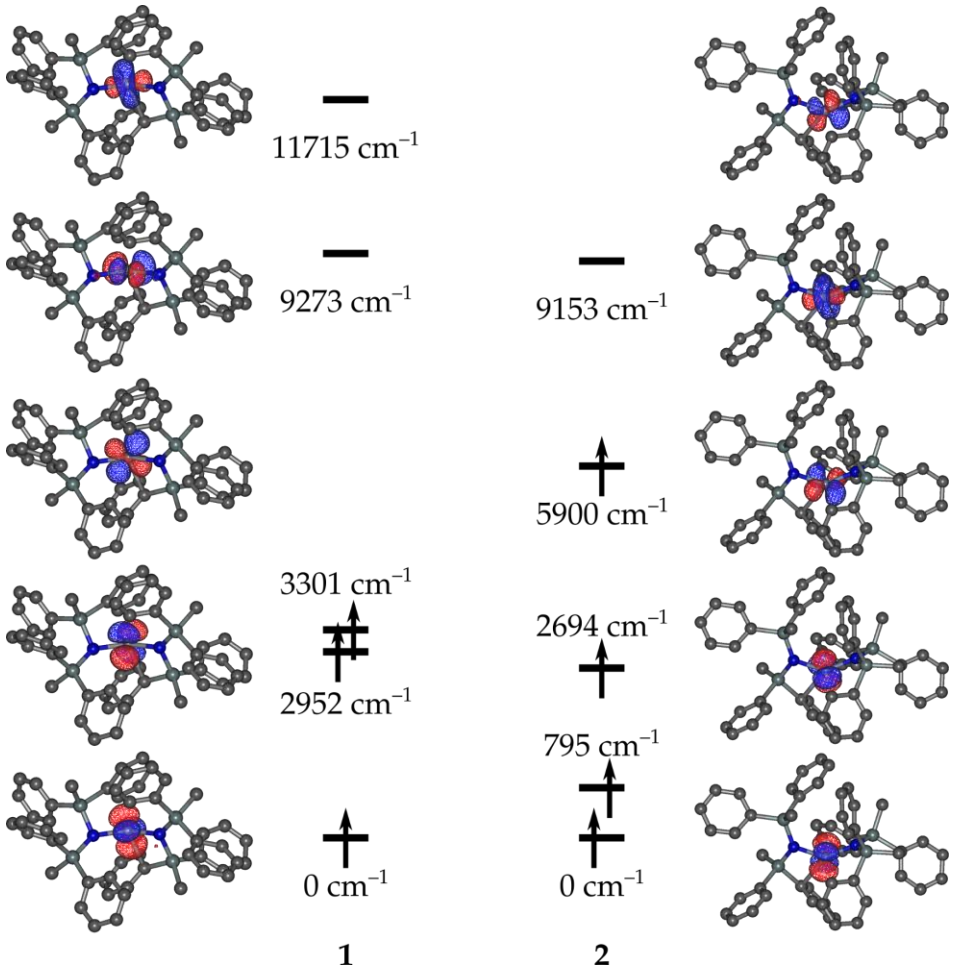

Figure 4. The effective ligand field 3*d* orbitals and orbital energies of V{N(SiMePh$_2$)$_2$}$_2$ (**1**) and Cr{N(SiMePh$_2$)$_2$}$_2$ (**2**) as calculated using *ab initio* ligand field theory. Hydrogen atoms are not shown for clarity.

Conclusion

In summary, the rare two-coordinate chromium and vanadium bis-silylamides Cr{N(SiMePh$_2$)$_2$}$_2$ (**1**) and V{N(SiMePh$_2$)$_2$}$_2$ (**2**) have been synthesized from their metal halide-THF precursors via salt metathesis. Both complexes have a bent coordination geometry (N-Cr-N 139.19(5) °, N-V-N 137.04(6) °) with secondary metal···C$_{Phenyl}$ interactions, which is also observed in the analogous iron(II) and cobalt (II) bis-silylamide complexes.[14] Magnetic studies afforded magnetic moments of 4.68 μ_B for **1** and 3.36 μ_B for **2**, which are both lower than the predicted spin-only values. This can be explained by weak second-order spin-orbit coupling effects arising from partially quenched orbital contribution to the angular momentum and the positive spin-orbit coupling constants of the less than half-filled 3*d* shells leading to partial cancellation of the spin and orbital moments. These observations were further corroborated by theoretical calculations.

Associated Content

Supporting Information

The Supporting Information, including spectra (infrared, UV-vis), SQUID measurements, crystallographic data, and computational methods and data is available free of charge on the ACS Publications website at DOI: xxxxxxxxx. CCDC entries 1060631 and 2010872 contain the supplementary crystallographic data of complexes 1 and 2. These data can be obtained free of charge via www.ccdc.cam.ac.uk/data_request/cif, or by emailing data_request@ccdc.cam.ac.uk, or by contacting The Cambridge Crystallographic Data Centre, 12 Union Road, Cambridge CB2 1EZ, UK; fax: + 44 1223 336033.

Author Information

Corresponding Author.

* roland.fischer@rub.de; *pppower@ucdavis.edu

ORCID

Cary R. Stennett: 0000-0002-2727-5747

Akseli Mansikkamäki: 0000-0003-0401-4373

Roland A. Fischer: 0000-0002-2727-5747

Philip P. Power: 0000-0002-6262-3209

ACKNOWLEDGMENT

This research was funded by the US National Science Foundation, Grant No. CHE-1565501. The dissertation project of K.F. was funded by the German Chemical Industry Fund (https://www.vci.de/fonds) and further supported by the RUB Research School (http://www.research.school.rub.de). CRS and PPP wish to acknowledge the US National Science Foundation (CHE-1565501) and AM acknowledges the Academy of Finland (grant no. 332294) and the University of Oulu (Kvantum Institute) for support of this work. The authors thank Dr. Eckhard Bill, MPI CEC, Mülheim, Germany, for SQUID measurements. Computational resources were provided by CSC-IT Center for Science in Finland and the Finnish Grid and Cloud Infrastructure (persistent identifier urn:nbn:fi:research-infras-2016072533).

References.

(1) Bürger, H.; Wannagat, U. Silylamido-Derivate von Eisen Und Kobalt. *Monatsh. Chem.* **1963**, *94*, 1007–1012.

(2) Bürger, H.; Wannagat, U. Silylamido-Verbindungen von Chrom, Mangan, Nickel Und Kupfer. *Monatsh. Chem.* **1964**, *95*, 1099–1102.

(3) Bradley, D. C.; Hursthouse, M. B.; Abdul Malik, K. M.; Möseler, R. The Crystal Molecular Structure of “Bis(Hexamethyldisilylamido) Manganese.” *Transit. Met. Chem.* **1978**, *3*, 253–254.

(4) Murray, B. D.; Power, P. P. Three-Coordinate Metal Amides of Manganese(II) and Cobalt(II): Synthesis and X-Ray Structure of the First Tris(Silylamide) of Manganese and the X-Ray Crystal Structures of $[M_2(N(SiMe_3)_2)_4]$ (M = Mn, Co). *Inorg. Chem.* **1984**, *23*, 4584–4588.

(5) Olmstead, M. M.; Power, P. P.; Shoner, S. C. Three-Coordinate Iron Complexes: X-Ray Structural Characterization of the Iron Amide-Bridged Dimers $[Fe(NR_2)_2]_2$ (R = $SiMe_3$, C_6H_5) and the Adduct $Fe[N(SiMe_3)_2]_2(THF)$ and Determination of the Association Energy of the Monomer $Fe\{N(SiMe_3)_2\}_2$ in Solution. *Inorg. Chem.* **1991**, *30*, 2547–2551.

(6) Ghotra, J. S.; Hursthouse, M. B.; Welch, A. J. Three-Co-Ordinate Scandium(III) and Europium(III); Crystal and Molecular Structures of Their Trishexamethyldisilylamides. *J. Chem. Soc., Chem. Commun.* **1973**, 669–670.

(7) Putzer, M. A.; Magull, J.; Goesmann, H.; Neumüller, B.; Dehnicke, K. Synthese, Eigenschaften Und Kristallstrukturen Der Titan(III)-Amido-Komplexe $Ti[N(SiMe_3)_2]_3$, $[TiCl_2\{N(SiMe_3)_2\}(THF)_2]$ Und $[Na(12\text{-Krone-}4)_2][TiCl_2\{N(SiMe_3)_2\}_2]$. *Chem. Ber.* **1996**, *129*, 1401–1405.

(8) Wagner, C. L.; Phan, N. A.; Fettinger, J. C.; Berben, L. A.; Power, P. P. New Characterization of $V\{N(SiMe_3)_2\}_3$: Reductions of Tris[Bis(Trimethylsilyl)Amido]Vanadium(III) and -Chromium(III) To Afford the Reduced Metal(II) Anions $[M\{N(SiMe_3)_2\}_3]^-$ (M = V and Cr). *Inorg. Chem.* **2019**, *58*, 6095–6101.

(9) Köhn, R. D.; Kociok-Köhn, G.; Haufe, M. The Chemistry of 1,3,5-Triazacyclohexane Complexes, 3. High Yield Synthesis of $[Cr\{N(SiMe_3)_2\}_3]$ and Accurate Structure Determination by Cocrystallization with Me_6Si_2. *Chem. Ber.* **1996**, *129*, 25–27.

(10) Ellison, J. J.; Power, P. P.; Shoner, S. C. First Examples of Three-Coordinate Manganese(III) and Cobalt(III): Synthesis and Characterization of the Complexes $M[N(SiMe_3)_2]_3$ (M = Mn or Co). *J. Am. Chem. Soc.* **1989**, *111*, 8044–8046.

(11) Hursthouse, M. B.; Rodesiler, P. F. Crystal and Molecular Structure of Tris(Hexamethyldisilylamido)Iron(III). *J. Chem. Soc. Dalton Trans.* **1972**, 2100–2102.

(12) Bartlett, R. A.; Power, P. P. Two-Coordinate, Nonlinear, Crystalline D6 and D7 Complexes: Syntheses and Structures of $M\{N(SiMePh_2)_2\}_2$, M = Fe or Co. *J. Am. Chem. Soc.* **1987**, *109*, 7563–7564.

(13) Chen, H.; Bartlett, R. A.; Dias, H. V. R.; Olmstead, M. M.; Power, P. P. The Use of Very Crowded Silylamide Ligands $-N(SiMenPh_{3-n})_2$(n = 0, 1, or 2) to Synthesize Crystalline, Two-Coordinate, Derivatives to Manganese(II), Iron(II), and Cobalt(II) and the Free Ion $[Ph_3SiNSiPh_3]^-$. *J. Am.*

Chem. Soc. **1989**, *111*, 4338–4345.

(14) Boynton, J. N.; Guo, J.-D.; Fettinger, J. C.; Melton, C. E.; Nagase, S.; Power, P. P. Linear and Nonlinear Two-Coordinate Vanadium Complexes: Synthesis, Characterization, and Magnetic Properties of V(II) Amides. *J. Am. Chem. Soc.* **2013**, *135*, 10720–10728.

(15) Cai, I. C.; Ziegler, M. S.; Bunting, P. C.; Nicolay, A.; Levine, D. S.; Kalendra, V.; Smith, P. W.; Lakshmi, K. V; Tilley, T. D. Monomeric, Divalent Vanadium Bis(Arylamido) Complexes: Linkage Isomerism and Reactivity. *Organometallics* **2019**, *38*, 1648–1663.

(16) Gerlach, C. P.; Arnold, J. Synthesis, Structure, and Reactivity of Three-Coordinate Vanadium(III) Chalcogenolates and Vanadium(V) Chalcogenide Chalcogenolates. *Inorg. Chem.* **1996**, *35*, 5770–5780.

(17) Ruppa, K. B. P.; Desmangles, N.; Gambarotta, S.; Yap, G.; Rheingold, A. L. Preparation and Characterization of a Homoleptic Vanadium(III) Amide Complex and Its Transformation into Terminal Chalcogenide Derivatives $[(3,5\text{-}Me_2Ph)AdN]_3VE$ (E = S, Se; Ad = Adamantyl). *Inorg. Chem.* **1997**, *36*, 1194–1197.

(18) Tran, B. L.; Singhal, M.; Park, H.; Lam, O. P.; Pink, M.; Krzystek, J.; Ozarowski, A.; Telser, J.; Meyer, K.; Mindiola, D. J. Reactivity Studies of a Masked Three-Coordinate Vanadium(II) Complex. *Angew. Chem. Int. Ed.* **2010**, *49*, 9871–9875.

(19) Tran, B. L.; Pinter, B.; Nichols, A. J.; Konopka, F. T.; Thompson, R.; Chen, C.-H.; Krzystek, J.; Ozarowski, A.; Telser, J.; Baik, M.-H.; Meyer, K.; Mindiola, D. J. A Planar Three-Coordinate Vanadium(II) Complex and the Study of Terminal Vanadium Nitrides from N_2: A Kinetic or Thermodynamic Impediment to N–N Bond Cleavage? *J. Am. Chem. Soc.* **2012**, *134*, 13035–13045.

(20) Cai, I. C.; Lipschutz, M. I.; Tilley, T. D. A Bis(Amido) Ligand Set That Supports Two-Coordinate Chromium in the +1, +2, and +3 Oxidation States. *Chem. Commun.* **2014**, *50*, 13062–13065.

(21) Nguyen, T.; Panda, A.; Olmstead, M. M.; Richards, A. F.; Stender, M.; Brynda, M.; Power, P. P. Synthesis and Characterization of Quasi-Two-Coordinate Transition Metal Dithiolates M(SAr*)2 (M = Cr, Mn, Fe, Co, Ni, Zn; Ar* = C_6H_3-2,6(C_6H_2-2,4,6-Pr^i_3)2. *J. Am. Chem. Soc.* **2005**, *127*, 8545–8552.

(22) König, S. N.; Schädle, C.; Maichle-Mössmer, C.; Anwander, R. Silylamide Complexes of Chromium(II), Manganese(II), and Cobalt(II) Bearing the Ligands $N(SiHMe_2)_2$ and $N(SiPhMe_2)_2$. *Inorg. Chem.* **2014**, *53*, 4585–4597.

(23) Bartlett, R. A.; Chen, H.; Power, P. P. [M(NMesBMes$_2$)$_2$] (M = Cr, Ni) : Stable, Distorted, Two-Coordinate d^4 and d^8 Complexes. *Angew. Chem. Int. Ed. English* **1989**, *28*, 316–317.

(24) Chen, H.; Bartlett, R. A.; Olmstead, M. M.; Power, P. P.; Shoner, S. C. Series of Two-Coordinate and Quasi-Two-Coordinate Transition-Metal Complexes: Synthesis, Structural, and Spectroscopic Studies of Sterically Demanding Borylamide Ligands -NRBR'$_2$ (R = Ph, R' = Mes, Xyl; R = R' = Mes), Their Lithium Salts, Li(Et$_2$O)$_2$NRBR'$_2$, . *J. Am. Chem. Soc.* **1990**, *112*, 1048–1055.

(25) Wolf, R.; Brynda, M.; Ni, C.; Long, G. J.; Power, P. P. Monomeric, Two-Coordinate, Univalent Chromium(I) Compounds: Steric Prevention of Metal−Metal Bond Formation. *J. Am. Chem. Soc.* **2007**, *129*, 6076–6077.

(26) Lei, H.; Guo, J.-D.; Fettinger, J. C.; Nagase, S.; Power, P. P. Two-Coordinate First Row Transition Metal Complexes with Short Unsupported Metal−Metal Bonds. *J. Am. Chem. Soc.* **2010**, *132*, 17399–17401.

(27) Boynton, J. N.; Merrill, W. A.; Reiff, W. M.; Fettinger, J. C.; Power, P. P. Two-Coordinate, Quasi-Two-Coordinate, and Distorted Three Coordinate, T-Shaped Chromium(II) Amido Complexes: Unusual Effects of Coordination Geometry on the Lowering of Ground State Magnetic Moments. *Inorg. Chem.* **2012**, *51*, 3212–3219.

(28) Power, P. P. Stable Two-Coordinate, Open-Shell (d^1–d^9) Transition Metal Complexes. *Chem. Rev.* **2012**, *112*, 3482–3507.

(29) Reiff, W. M.; LaPointe, A. M.; Witten, E. H. Virtual Free Ion Magnetism and the Absence of Jahn−Teller Distortion in a Linear Two-Coordinate Complex of High-Spin Iron(II). *J. Am. Chem. Soc.* **2004**, *126*, 10206–10207.

(30) Reiff, W. M.; Schulz, C. E.; Whangbo, M.-H.; Seo, J. I.; Lee, Y. S.; Potratz, G. R.; Spicer, C. W.; Girolami, G. S. Consequences of a Linear Two-Coordinate Geometry for the Orbital Magnetism and Jahn−Teller Distortion Behavior of the High Spin Iron(II) Complex Fe[N(*t*-Bu)$_2$]$_2$. *J. Am. Chem. Soc.* **2009**, *131*, 404–405.

(31) Merrill, W. A.; Stich, T. A.; Brynda, M.; Yeagle, G. J.; Fettinger, J. C.; De Hont, R.; Reiff, W. M.; Schulz, C. E.; Britt, R. D.; Power, P. P. Direct Spectroscopic Observation of Large Quenching of First-Order Orbital Angular Momentum with Bending in Monomeric, Two-Coordinate Fe(II) Primary Amido Complexes and the Profound Magnetic Effects of the Absence of Jahn− and Renner−Teller Distortions In. *J. Am. Chem. Soc.* **2009**, *131*, 12693–12702.

(32) Zadrozny, J. M.; Atanasov, M.; Bryan, A. M.; Lin, C.-Y.; Rekken, B. D.; Power, P. P.; Neese, F.; Long, J. R. Slow Magnetization Dynamics in a Series of Two-Coordinate Iron(II) Complexes. *Chem. Sci.* **2013**, *4*, 125–138.

(33) Bryan, A. M.; Merrill, W. A.; Reiff, W. M.; Fettinger, J. C.; Power, P. P. Synthesis, Structural, and Magnetic Characterization of Linear and Bent Geometry Cobalt(II) and Nickel(II) Amido

Complexes: Evidence of Very Large Spin–Orbit Coupling Effects in Rigorously Linear Coordinated Co^{2+}. *Inorg. Chem.* **2012**, *51*, 3366–3373.

(34) Rinehart, J. D.; Fang, M.; Evans, W. J.; Long, J. R. A N_2^{3-} Radical-Bridged Terbium Complex Exhibiting Magnetic Hysteresis at 14 K. *J. Am. Chem. Soc.* **2011**, *133*, 14236–14239.

(35) Harriman, K. L. M.; Brosmer, J. L.; Ungur, L.; Diaconescu, P. L.; Murugesu, M. Pursuit of Record Breaking Energy Barriers: A Study of Magnetic Axiality in Diamide Ligated DyIII Single-Molecule Magnets. *J. Am. Chem. Soc.* **2017**, *139*, 1420–1423.

(36) Ungur, L.; Le Roy, J. J.; Korobkov, I.; Murugesu, M.; Chibotaru, L. F. Fine-Tuning the Local Symmetry to Attain Record Blocking Temperature and Magnetic Remanence in a Single-Ion Magnet. *Angew. Chem. Int. Ed.* **2014**, *53*, 4413–4417.

(37) Guo, F.-S.; Day, B. M.; Chen, Y.-C.; Tong, M.-L.; Mansikkamäki, A.; Layfield, R. A. Magnetic Hysteresis up to 80 Kelvin in a Dysprosium Metallocene Single-Molecule Magnet. *Science* **2018**, *362*, 1400 LP – 1403.

(38) Figgis, B. N. *Introduction to Ligand Fields.*; New York, Interscience Publishers: New York, 1966.

(39) Pyykkö, P.; Atsumi, M. Molecular Single-Bond Covalent Radii for Elements 1–118. *Chem. – A Eur. J.* **2009**, *15*, 186–197.

(40) Niemeyer, M. Synthesis and Structural Characterization of Several Ytterbium Bis(Trimethylsilyl)Amides Including Base-Free $[Yb\{N(SiMe_3)_2\}_2(\mu\text{-}Cl)]_2$ — A Coordinatively Unsaturated Complex with Additional Agostic Yb···(H_3C—Si) Interactions. *Z. Anorg. Allg. Chem.* **2002**, *628*, 647–657.

(41) Bradley, D. C.; Hursthouse, M. B.; Ibrahim, A. A.; Malik, K. M. A.; Motevalli, M.; Möseler, R.; Powell, H.; Runnacles, J. D.; Sullivan, A. C. Synthesis and Chemistry of the Bis(Trimethylsilyl)Amido Bis-Tetrahydrofuranates of the Group 2 Metals Magnesium, Calcium, Strontium and Barium. X-Ray Crystal Structures of $Mg[N(SiMe_3)_2]_2{\cdot}2THF$ and Related $Mn[N(SiMe_3)_2]_2{\cdot}2THF$. *Polyhedron* **1990**, *9*, 2959–2964.

(42) Kern, R. J. Tetrahydrofuran Complexes of Transition Metal Chlorides. *J. Inorg. Nucl. Chem.* **1962**, *24*, 1105–1109.

(43) Hitchcock, P. B.; Hughes, D. L.; Leigh, G. J.; Sanders, J. R.; De Souza, J.; McGarry, C. J.; Larkworthy, L. F. Preparation of New Vanadium(II) Iodides and Crystal Structure of Hexakis(Acetonitrile)Vanadium(II)(Tetraiodide). *J. Chem. Soc. Dalton Trans.* **1994**, No. 24, 3683–3687.

(44) CrysAlisPRO. Oxford Diffraction/Agilent Technologies UK Ltd, Yarnton, England.

(45) SCALE3 ABSPACK. Oxford Diffraction Ltd. 2005.

(46) Sheldrick, G. M. A Short History of *SHELX*. *Acta Crystallogr. Sect. A* **2008**, *64*, 112–122.

(47) Bain, G. A.; Berry, J. F. Diamagnetic Corrections and Pascal's Constants. *J. Chem. Educ.* **2008**, *85*, 532.

(48) Drago, R. S. *Physical Methods for Chemists*, 2nd ed..; Drago, R. S., Ed.; Gainesville, Fla. : Surfside Scientific Publishers: Gainesville, Fla., 1992.

(49) Roos, B. O. The Complete Active Space Self-Consistent Field Method and Its Applications in Electronic Structure Calculations. *Advances in Chemical Physics*. January 1, 1987, pp 399–445.

(50) Siegbahn, P.; Heiberg, A.; Roos, B.; Levy, B. A Comparison of the Super-CI and the Newton-Raphson Scheme in the Complete Active Space SCF Method. *Phys. Scr.* **1980**, *21*, 323–327.

(51) Roos, B. O.; Taylor, P. R.; Sigbahn, P. E. M. A Complete Active Space SCF Method (CASSCF) Using a Density Matrix Formulated Super-CI Approach. *Chem. Phys.* **1980**, *48*, 157–173.

(52) Siegbahn, P. E. M.; Almlöf, J.; Heiberg, A.; Roos, B. O. The Complete Active Space SCF (CASSCF) Method in a Newton–Raphson Formulation with Application to the HNO Molecule. *J. Chem. Phys.* **1981**, *74*, 2384–2396.

(53) Angeli, C.; Cimiraglia, R.; Evangelisti, S.; Leininger, T.; Malrieu, J.-P. Introduction of N-Electron Valence States for Multireference Perturbation Theory. *J. Chem. Phys.* **2001**, *114*, 10252–10264.

(54) Angeli, C.; Cimiraglia, R.; Malrieu, J.-P. N-Electron Valence State Perturbation Theory: A Fast Implementation of the Strongly Contracted Variant. *Chem. Phys. Lett.* **2001**, *350*, 297–305.

(55) Angeli, C.; Cimiraglia, R.; Malrieu, J.-P. N-Electron Valence State Perturbation Theory: A Spinless Formulation and an Efficient Implementation of the Strongly Contracted and of the Partially Contracted Variants. *J. Chem. Phys.* **2002**, *117*, 9138–9153.

(56) Singh, S. K.; Atanasov, M.; Neese, F. Challenges in Multireference Perturbation Theory for the Calculations of the G-Tensor of First-Row Transition-Metal Complexes. *J. Chem. Theory Comput.* **2018**, *14*, 4662–4677.

(57) Atanasov, M.; Ganyushin, D.; Sivalingam, K.; Neese, F. A Modern First-Principles View on Ligand Field Theory Through the Eyes of Correlated Multireference Wavefunctions BT - Molecular Electronic Structures of Transition Metal Complexes II; Mingos, D. M. P., Day, P., Dahl, J. P., Eds.; Springer Berlin Heidelberg: Berlin, Heidelberg, 2012; pp 149–220.

(58) Singh, S. K.; Eng, J.; Atanasov, M.; Neese, F. Covalency and Chemical Bonding in Transition Metal Complexes: An Ab Initio Based Ligand Field Perspective. *Coord. Chem. Rev.* **2017**, *344*, 2–

TOC Image:

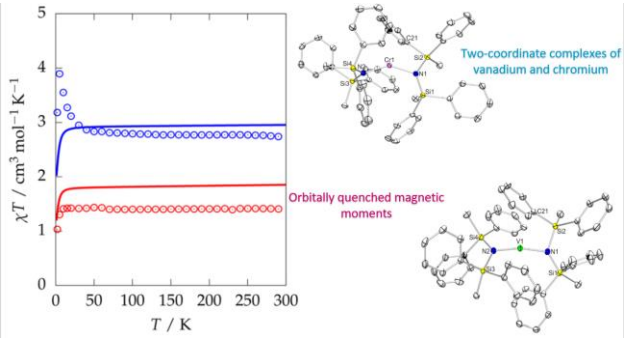

Synopsis:

This work describes the synthesis of rare homoleptic, two-coordinate complexes of vanadium and chromium featuring the silylamide ligand -N(SiMePh$_2$)$_2$. Both feature bent geometry and secondary interactions with a ligand aryl carbon. Magnetic and computational studies showed that spin-orbit coupling resulted in quenching of their magnetic moments to below the spin only value in contrast to the increased magnetic moments found in complexes with greater than half-filled valence shells.